such as losses of HPO_3 (-80 Da) and HPO_4 (-96 Da). The MS/MS spectrum of phosphorylated [Tyr^5]bradykinin (Figure 5) contained definitive fragment ions that clearly identified phosphotyrosine and its sequence position. The peak at m/z 216 is the immonium ion fragment of a phosphoryltyrosine residue, $CH(CH_2C_5H_4OPO_3H_2)=NH_2^+$, and has been observed in other MS/MS spectra of phosphotyrosine-containing peptides.[30,31] One also observes significant fragment ions for $(M + H - HPO_3)^+$ and $(M + H - H_2PO_3)^+$, which is observed primarily as $(M + H - H_3PO_4)^+$ in peptides containing phosphoserine.[36]

Conclusions

The importance of tyrosine kinase activity associated with growth factor receptors and oncogenic and protooncogenic protein products is well established. To study this important class of enzymes in more detail, more versatile and efficient synthetic methods for the preparation of peptides and peptide analogues containing phosphotyrosine need to be developed. Some of these peptides may find use as product inhibitors of these tyrosyl protein kinase enzymes, leading to their development as pharmaceuticals. In addition, a synthetic route for phostyrosine-containing peptides will undoubtedly be essential to determine the substrate specificity of the associated tyrosine phosphatase enzymes.

The strategy described here provides an efficient route in the synthesis of phosphotyrosine-containing peptides directly from their parent nonphosphorylated peptides. The conversion of the adenylylated peptide intermediates by either treatment with micrococcal nuclease (a commercially available enzyme) or oxidative degradation with sodium periodate has been found to be virtually quantitative, with very little side product formation. The transfer of AMP to peptide substrates catalyzed by ATase is versatile and highly specific for tyrosine moieties. Although ATase is not commerically available, it has reportedly been overproduced to levels approaching 500-fold in *E. coli* using the plasmid vector pKC30.[37] It is also the only available method that can work on intact peptides with selectivity for tyrosine residues. It is encouraging that all peptides that have been subjected to the ATase treatment have been adenylylated to some extent (≥3%), although this may not have been the case for the second tyrosine (Tyr-11) in neurotensin. In this latter case, it is not clear whether Tyr-11 is a poor substrate or if the relatively faster adenylylation of Tyr-3, whose neighboring amino acids resemble those in glutamine synthetase, occurs to such an extent as to preclude adenylylation of the second tyrosine.

It may be possible to increase significantly this reaction yield by coupling the conversion of the adenylylated intermediate to the formation of its phosphotyrosine product by finding conditions where both ATase and micrococcal nuclease can function simultaneously. We are currently exploring this possibility along with immobilization of both enzymes with the aim of finding conditions that will yield a quantitative overall conversion to the phosphotyrosine peptide product. Beside the obvious importance of a synthetic strategy for phosphotyrosine peptides, the production of the corresponding adenylylated tyrosine analogues also has some interesting implications. For example, peptides containing adenylylated tyrosine may find use as bisubstrate inhibitors of tyrosine kinases, as they incorporate potential binding features of both ATP and tyrosine-containing substrates.

Acknowledgment. We would like to thank Dr. S. G. Rhee (NIH at Bethesda) for the generous gift of ATase and Dr. J. McMurray (The University of Texas, Houston) for the synthesis of GS-17. We would also like to acknowledge the financial support of the Bristol Meyers Co. and grants from the National Cancer Institute (CA 37655, G.L.K.), National Institutes of Health (RR01614, B.W.G.; GM 23529, J.J.V.), and National Science Foundation Biological Instrumentation Division (DIR 8700766, A. L. Burlingame).

(36) Biemann, K.; Scoble, S. A. *Science* **1987**, *238*, 992-998.

(37) Rhee, S.; Chock, P.; Stadtman, E. In *Advances in Enzymology and Related Areas of Molecular Biology*; Meister, A., Ed.; Wiley: New York, 1989, Vol. 62, pp 37-92.

Laser Photochemistry of DNA: Two-Photon Absorption and Optical Breakdown Using High-Intensity, 532-nm Radiation

Y. Hefetz,[†] D. A. Dunn,[†] T. F. Deutsch,[†] L. Buckley,[†] F. Hillenkamp,[‡] and I. E. Kochevar*,[†]

Contribution from the Wellman Laboratories, Department of Dermatology, Massachusetts General Hospital, Harvard Medical School, Boston, Massachusetts 02114, and Institute for Medical Physics, University of Muenster, D-4400 Muenster, FRG. *Received April 30, 1990*

Abstract: Formation of cyclobutylpyrimidine dimers and strand breaks in double-stranded DNA was investigated by using 532-nm, 28-ps pulses from a frequency-doubled, mode-locked Nd:YAG laser at intensities below and above the threshold for optical breakdown. Two-photon absorption by DNA was detected in the absence of optical breakdown by measuring the yields of cyclobutylpyrimidine dimers formed in supercoiled pBR322 DNA. The yield of cyclobutylpyrimidine dimers per laser pulse was measured at seven peak intensities between 1.03 and 8.04 GW/cm^2. A plot of the ln (dimer yield/pulse) versus ln (photon flux) was linear with a slope of 1.88 ± 0.26. The two-photon cross section for absorption at 532 nm was calculated to be 0.5 (±0.2) × 10^{-52} cm^4 s photon^{-1} per nucleotide. Experiments performed by using intensities above the threshold for optical breakdown caused breaks in the DNA strands but no cyclobutylpyrimidine dimers. The free-radical quencher, mannitol, partially inhibited formation of the strand breaks, indicating that mechanical processes initiated by the plasma also contribute to the creation of DNA strand breaks.

Intensity-dependent laser photochemistry of organic molecules has received increasing attention recently.[1-3] Most of these studies have involved sequential two-photon absorption; the first photon is absorbed by the ground state and the second by an electronically excited state, usually the triplet, or a transient intermediate. In some cases, a molecule in an upper excited state reacts prior to relaxation to the lowest excited state of that manifold.[2] Absorption

[†] Harvard Medical School.
[‡] University of Muenster.

(1) (a) Lachish, U.; Shafferman, A.; Stein, G. *J. Chem. Phys.* **1976**, *64*, 4205-4212. (b) Turro, N. J.; Aikawa, M.; Butcher, J. A.; Griffin, G. W. *J. Am. Chem. Soc.* **1980**, *102*, 5127-5128. (c) McGimpsey, W. C.; Scaiano, J. C. *Chem. Phys. Lett.* **1987**, *138*, 13-17. (d) Jent, F.; Paul, H.; Fischer, H. *Chem. Phys. Lett.* **1988**, *146*, 315-319.

0002-7863/90/1512-8528$02.50/0

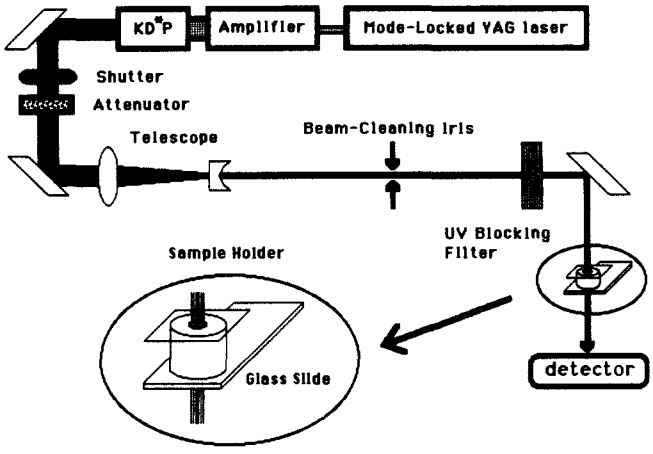

Figure 1. Schematic diagram of the experimental setup for 532-nm irradiation of DNA solutions. The frequency-doubled, mode-locked Nd:YAG laser produced 28 ps-long, 532-nm pulses. The beam is spatially filtered and reduced in diameter to irradiate the sample in a 1.5-mm-diameter sample holder. The intensity was controlled with attenuators.

by other transient species such as radicals can also lead to intensity-dependent photoproduct formation.[3] Previous reports of intensity-dependent photochemistry of biological molecules has focused mainly on 266- and 248-nm pulsed laser radiation effects on DNA, nucleic acid bases, and aromatic amino acids.[4,5] The change in product distribution from that obtained with low-intensity sources was attributed to sequential two-photon absorption within the singlet manifold when picosecond-long pulses (I = 4 GW/cm^2) were used and to absorption of a second photon by the triplet state using an intensity of 5 MW/cm^2 from a nanosecond-pulsed laser.[5] Intensity-dependent photosensitization in biological systems has been reported and may be important in the development of therapeutic agents.[6]

Two-photon absorption at wavelengths for which there is no monophotonic transition has been studied by use of high-peak-power laser sources.[7,8] Values of two-photon absorption cross sections for organic molecules are typically 10^{-49}–10^{-51} cm^4 s photon^{-1} and have been obtained largely from measurements based on fluorescence.[9] Two-photon fluorescence excitation spectroscopy is used to locate excited-state energy levels that, because of selection rules, are not accessible by one-photon excitation.[7] Photochemical effects of simultaneous two-photon absorption have only infrequently been reported.[8,10]

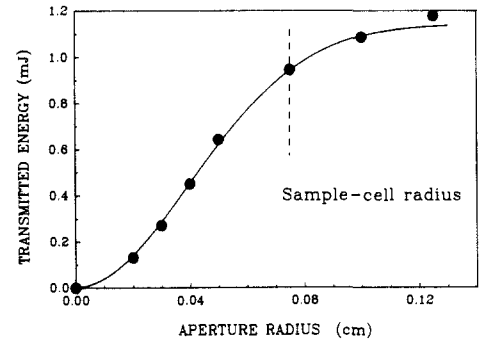

Figure 2. Energy per pulse arriving at the detector after passing through an aperture inserted in the beam. The solid line is a theoretical fit describing the transmitted energy for a Gaussian beam of 0.954-nm FWHM and 109 mJ/cm^2 at the center.

Laser-induced optical breakdown is currently used in ophthamology where the intensities in the eye exceed 1 GW/cm^2. Other medical applications of high-peak-power lasers are under development.[11] Use of very high intensities in medicine introduces the possibility that photoproducts may be formed in tissue as a result of nonresonant two-photon absorption. In effect, infrared photons could initiate photochemistry of visible-absorbing chromophores and visible photons could cause photoreactions in UV-absorbing species.

We investigated the effect of high-peak-power, short-pulse visible laser radiation on UV-absorbing DNA because of the critical role of this macromolecule in cells. The UV-induced photochemistry of DNA has been well studied, the major photoproducts being cyclobutylpyrimidine dimers which, along with (6–4) pyrimidine–pyrimidone dimers, are the major cytotoxic and mutagenic photoproducts in cells.[12,13] Breaks in the DNA backbone are photochemically initiated with low quantum yield when DNA is excited by low-intensity UV[4f,14] but are more efficiently produced by photosensitization mechanisms.[15]

We report here a two-photon absorption cross section for DNA at 532 nm that is based on measurements of the yield of cyclobutylpyrimidine dimers produced using 28-ps, 532-nm pulses from a mode-locked, frequency-doubled Nd:YAG laser. In addition, we show that laser-induced optical breakdown (plasma formation) causes breaks in the DNA strands by mechanisms involving radicals and mechanical effects.

Experimental Section

Picosecond Irradiation without Optical Breakdown. Figure 1 shows a schematic diagram of the experimental apparatus. An active–passive mode-locked, Nd:YAG laser with single-pulse selection (Quantel YG 501-10) was used. Frequency doubling using a KDP crystal resulted in 28-ps-long full width at half-maximum intensity (FWHM), 532-nm pulses at 10 Hz. A set of neutral density filters was used to control the peak intensity at the sample (1.03–8.04 GW/cm^2; 0.96–7.52 mJ/pulse). The beam, 0.8 cm in diameter, was passed through a beam-reducing telescope and cleaned by a metal aperture used as a spatial filter. The collimated beam was passed vertically through a 0.15-cm-diameter, 1-

(2) (a) Andreoni, A.; Cubeddu, R.; De Silvestri, S.; Laporta, P.; Svelto, O. *Phys. Rev. Lett.* **1980**, *45*, 431–433. (b) Andreoni, A.; Cubeddu, R.; Svelto, O.; Canti, G.; Ricci, L.; Smilguiavitchious, V. *Lasers Life Sci.* **1987**, *1*, 213–218. (c) Johnston, L. J.; Scaiano, J. C. *J. Am. Chem. Soc.* **1987**, *109*, 5487–5491. (d) Beuttner, G. R.; Hall, R. D.; Chignell, C. R.; Motten, A. G. *Photochem. Photobiol.* **1989**, *49*, 249–256.

(3) Scaiano, J. C.; Wagner, P. J. *J. Am. Chem. Soc.* **1984**, *106*, 4626–4627.

(4) (a) Angelov, D. A.; Kryukov, P. G.; Letokhov, V. S.; Nikogosyan, D. N.; Oraevskii, A. A. *Appl. Phys.* **1980**, *21*, 391–395. (b) Schulte-Frohlinde, D.; Opitz, J.; Gorner, H.; Bothe, E. *Int. J. Radiat. Biol.* **1985**, *48*, 397–408. (c) Budowsky, E. I.; Kovalsky, O. I.; Yakovlev, D. Y.; Simukova, N. A.; Rubin, L. B. *FEBS Lett.* **1985**, *188*, 155–158. (d) Oraevsky, A. A.; Nikogosyan, D. N. *Chem. Phys.* **1985**, *100*, 429–445. (e) Kozlov, A. A.; Lobko, V. V.; Matveetz, Y. A.; Nikogosyan, D. N.; Letokhov, V. S. *Lasers Life Sci.* **1987**, *1*, 247–264. (f) Opitz, J.; Schulte-Frohlinde, D. *J. Photochem.* **1987**, *39*, 145–163. (g) Masnyk, T. W.; Nguyen, H. T.; Minton, K. W. *J. Biol. Chem.* **1989**, *264*, 2482–2488.

(5) Zavilgelsky, G. B.; Gurzadyan, G. G.; Nikogosyan, D. N. *Photobiochem. Photobiophys.* **1984**, *8*, 175–187.

(6) (a) Gurzadyan, G. G.; Nikogosyan, D. N.; Kryukov, P. G.; Letokhov, V. S.; Balmukhanov, T. S.; Belogurov, A. A.; Zavilgelskij, G. B. *Photochem. Photobiol.* **1981**, *33*, 835–838. (b) Andreoni, A.; Cubeddu, R.; De Silvestri, S.; Laporta, P.; Ambesi-Impiombato, R. S.; Esposito, M.; Mastrocinque, M.; Tramontano, D. *Cancer Res.* **1983**, *43*, 2076–2080. (c) Shea, C. R.; Long, F.; Deutsch, T.; Hasan, T. *Lasers Life Sci.* **1988**, *2*, 29–38. (d) Fluhler, E. N.; Hurley, J. K.; Kochevar, I. E. *Biochim. Biophys. Acta* **1989**, *990*, 269–275. (e) Shea, C. R.; Hefetz, Y.; Gillies, R.; Wimberly, J.; Dalickas, G.; Hasan, T. *J. Biol. Chem.* **1990**, *265*, 5977–5982.

(7) Worlock, J. M. In *Laser Handbook*; Arecchi, F. T., Schulz-Dubois, E. O., Eds.; North-Holland: Amsterdam, 1972; pp 1323–1370, and references therein.

(8) Jiang, S. P. *Prog. React. Kinet.* **1989**, *15*, 77–82.

(9) Birks, J. B. *Photophysics of Aromatic Molecules*; Wiley-Interscience: London, 1970; pp 62–83.

(10) Rounds, D. E.; Olson, R. S.; Johnson, F. M. *NEREM Rec.* **1966**, 158–159.

(11) (a) Zysset, B.; Fujimoto, J. G.; Puliafito, C. A.; Birngruber, R.; Deutsch, T. F. *Lasers Surg. Med.* **1989**, *9*, 193–204, and references therein. (b) Zysset, B.; Fujimoto, J. G.; Deutsch, T. F. *Appl. Phys. B* **1989**, *48*, 139–147, and references therein.

(12) Patrick, M. H.; Rahn, R. O. In *Photochemistry and Photobiology of Nucleic Acids*; Wang, S. Y., Ed.; Academic Press: New York, 1976; Vol. II, pp 35–96.

(13) Cleaver, J. E.; Cortes, F.; Karentz, D.; Lutze, L. H.; Morgan, W. F.; Player, A. N.; Vuksanovic, L.; Mitchell, D. L. *Photochem. Photobiol.* **1988**, *48*, 41–49.

(14) Kochevar, I. E.; Buckley, L. A. *Photochem. Photobiol.* **1990**, *51*, 527–532.

(15) (a) Piette, J.; Merville-Louis, M. P.; Decuyper, J. *Photochem. Photobiol.* **1986**, *44*, 793–802. (b) Cadet, J.; Berger, M.; Decarroz, C.; Wagner, J. R.; Van Lier, J. E.; Ginot, Y. M.; Vigny, P. *Biochimie* **1986**, *68*, 813–834. (c) Kochevar, I. E.; Dunn, D. A. In *Bio-Organic Photochemistry*; Morrison, H., Ed.; Wiley-Interscience: New York, 1990; Vol. 1, pp 273–315.

cm-long glass capillary tube, which served as a sample holder. A long-pass absorption filter placed immediately before the sample ensured that no UV radiation reached the sample. After spatial filtering the beam profile was approximately Gaussian, as determined by methods described below. The energy/pulse incident on the sample was measured with a joulemeter (Molectron J-25). Several checks, ranging from visual observation through a 532-nm blocking filter to measurements using a Si detector coupled to a pulse counter, were used to ensure that the irradiation conditions did not produce optical breakdown. A shutter controlled by a pulse counter determined the irradiation time. All irradiations were at room temperature. No effort was made to exclude oxygen during any of the irradiations. The DNA solution was covered with a thin glass cover slip to prevent evaporation during the exposure and was carefully observed to reject samples having air bubbles in the optical path. Laser pulse duration was calculated at 532 nm from autocorrelation measurements of the fundamental (1064 nm) radiation.[16]

Because two-photon absorption is a nonlinear process, the beam profile must be known if quantitative results are to be obtained. The output laser beam was not the Gaussian TEM_{00} mode; thermal lensing and gain inhomogencities in the amplifier rod produce a distorted flat top beam with concentric diffraction rings. With the optical system shown in Figure 1, the far-field diffraction pattern at the sample plane (2.25 m from the telescope) approximates an Airy disk with (FWHM) diameter of 0.0954 cm.[17]

Several measurements were made to document the beam profile. A set of burn patterns taken at the position of the sample and examined with a microscope did not show any hot spots. The energy transmitted through calibrated apertures of different sizes was measured and compared to that predicted for a Gaussian beam truncated by an aperture.[16] The results are shown in Figure 2; the central part of the beam follows the behavior of a Gaussian beam with diameter $2R = 0.0954$-cm FWHM and fluence 109 mJ/cm^2 at the center.

Aqueous solutions of supercoiled pBR322 DNA (sc-DNA), which were 7.8×10^{-5} M in nucleotides (25 ng/μL, 30 μL), were irradiated. A series of experiments was performed using seven peak intensities between 1.03 and 8.04 GW/cm^2. At each intensity, samples were exposed to varying numbers of laser pulses. The maximum number of laser pulses varied from 905 at the highest intensity to 54 306 at the lowest intensity. The maximum total energy delivered to a sample was between 3.6 and 27.7 J. Because of the small two-photon absorption cross section for DNA at 532 nm, even the highest delivered dose produced less than 20% decrease in the supercoiled DNA.

Continuous-Wave Irradiations. Experiments were performed to determine whether low-intensity visible radiation affected pBR322 DNA. The collimated laser beam at 514 nm from an argon ion laser was used to expose solutions of sc-DNA (7.8×10^{-5} M nucleotides) in the same capillary used for the picosecond laser irradiations described above. The intensity was 3.0 W/cm^2 and samples were irradiated for five different times. The longest exposure delivered 200 J, which was considerably higher than the highest total energy delivered in the picosecond-irradiation experiments.

Picosecond Irradiation above the Threshold for Optical Breakdown. To examine the effects of laser-induced optical breakdown (plasma formation) on solutions of DNA, the 532-nm beam of the picosecond Nd:YAG laser was focused within a solution of pBR322 DNA by use of a 1-in. focal-length lens. The spot size at the focus was calculated to be ~ 5 μm. For the 2 mJ/pulse energies typically used in this set of experiments the intensity at the focus would be 360 TW/cm^2 (3.6×10^{14} W/cm^2), well above typical values for optical breakdown in water. The optical breakdown threshold for water depends on purity as well as spot size and pulse width;[18] typical values measured with our system using 1.06-μm pulses ranged from 0.5 to 1.6 TW/cm^2.[11a] The high irradiances used assured reliable occurrence of breakdown on each pulse.

The sc-DNA sample (3.12×10^{-5} M nucleotides, 10 ng/μL, 200 μL) in a microtest tube (0.35 cm × 3 cm) was stirred with a magnetic flea. The focal point was ~ 0.1 cm beneath the surface and 0.9 cm above the top of the magnetic flea. Varying numbers of pulses were delivered to each sample; the maximum cummulative energy delivered was 7 J. In some experiments, varying concentrations of mannitol or sodium azide were present during the exposure to evaluate the role of free radicals in the formation of strand breaks.

Analysis for DNA Photoproducts. Supercoiled plasmid pBR322 DNA (sc-DNA, Boehringer Mannheim Biochemical) was used because a single-strand break converts a sc-DNA molecule into a relaxed form (rel-DNA) of the molecule, and these two forms are readily separated by agarose gel electrophoresis. Concentrations of pBR322 DNA (92–95% supercoiled as received) were calculated by using a molecular mass of 2.8×10^6 daltons. Cyclobutylpyrimidine dimers were quantitated by treating half of each sample with dimer-specific *Micrococcus luteus* UV endonuclease (Applied Genetics, Freeport, NY), which cleaves DNA strands at sites of cyclobutylpyrimidine dimers. Samples were incubated with enzyme (2 units/ng of DNA) for 30 min at 37 °C in buffer (30 mM Tris, 40 mM NaCl, and 1 mM EDTA, pH 8). The other half of each sample was not treated with enzyme and, thus, was used to measure the number of strand breaks present before the irradiation plus those introduced during the treatment.

The enzyme-treated and untreated samples were run on the same neutral agarose electrophoresis gel. Electrophoresis was performed as described previously.[19] Briefly, samples were analyzed on 1% neutral agarose gels (type II agarose, Sigma Chemical Co., St. Louis, MO) in a Bio-rad Mini-Sub cell apparatus. Gels were stained with ethidium bromide, the fluorescence of the intercalated dye was photographed with a Polaroid MPF camera, and photographs of the gels were scanned with a densitometer in reflectance mode at 550 nm. The integrated areas under the sc-DNA and rel-DNA peaks were used to calculate the fraction of sc-DNA (f_{sc}) in the sample. The area of the peak for rel-DNA was divided by 1.66 to correct for the greater binding of ethidium bromide to rel-DNA compared to sc-DNA.[19] The decrease in f_{sc} resulting from dimer formation was calculated by subtracting the f_{sc} value for untreated samples from the f_{sc} value for the paired, UV-endonuclease-treated sample.

Results and Discussion

Formation of Cyclobutylpyrimidine Dimers Using 532-nm, Picosecond Laser Radiation. The content of cyclobutylpyrimidine dimers (henceforth called dimers) was measured in samples of sc-pBR322 DNA that were exposed to varying numbers of laser pulses using seven peak intensities. As discussed in the Experimental Section, introduction of one (or more) dimer into a sc-DNA molecule is detected by the conversion of one molecule of sc-DNA into the rel-DNA form upon treatment with UV endonuclease. Therefore, with increasing numbers of laser pulses, the fraction of DNA remaining as sc-DNA (f_{sc}) decreases. In order to determine whether two-photon absorption was responsible for the formation of dimers, the relationship between the laser intensity and the rates of dimer formation was analyzed.

With a collimated laser beam and an optically thin sample, the photon flux, F, (in photons s^{-1} cm^{-2}) can be regarded to be a function of only the time, t, and the distance from the capillary center, r. The assumption of an optically thin sample is reasonable even at the highest intensities used in these experiments because of the low values for two-photon cross sections. Assuming that mixing occurs during the experiment, the [sc-DNA] is uniform throughout the sample. The rate at which the fraction of sc-DNA, f_{sc}, decreases is given by

$$df_{sc}/dt = -f_{sc}[\sigma_1\phi_1 F(r,t) + \sigma_2\phi_2 F^2(r,t)] \quad (1)$$

where σ_1 is the one-photon cross section (in cm^2), σ_2 is the two-photon cross section (in cm^4 s photon^{-1}), and Φ_1 and Φ_2 are the quantum yields for production of a dimer following absorption of one or two photons, respectively. The contribution of monophotonic absorption to dimer formation is exceedingly small because DNA does not absorb at 532 nm; thus, eq 1 can be integrated to give

$$\ln [f_{sc}(t)] - \ln [f_{sc}(t=0)] = \frac{-\sigma_2\phi_2}{\pi R_o^2}\int_0^t dt' \int_0^{R_o} F^2(r,t')2\pi r\, dr \quad (2)$$

where the integration is carried out over the total exposure duration, t, of N pulses and R_o is the radius of the cuvette. Defining the average photon flux during the laser pulse as

$$\bar{F} = \frac{E/h\nu}{\pi R_o^2 \tau_p} \quad (3)$$

(16) Siegman, A. E. In *Lasers*; University Science Books: Mill Valley, CA, 1986; p 1081.
(17) Lipson, S. G.; Lipson, H. In *Optical Physics*; University Press: Cambridge, U.K., 1969; pp 185–199.
(18) Docchio, F.; Sacchi, C. A.; Marshall, J. *Lasers Ophthalmol.* **1986**, *7*, 83–93.
(19) Ciulla, T. A.; Van Camp, J. R.; Rosenfeld, E.; Kochevar, I. E. *Photochem. Photobiol.* **1989**, *49*, 293–299.

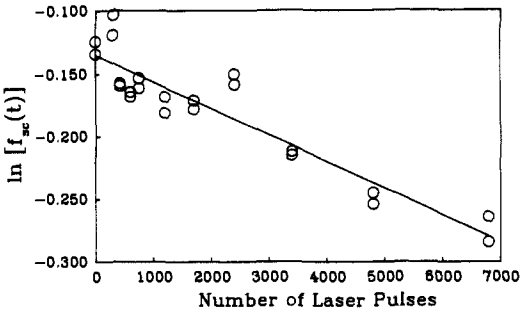

Figure 3. The ln fractional amount of sc-DNA (f_{sc}) remaining after delivery of varying numbers of 532-nm, 28-ps pulses to pBR322 DNA. The f_{sc} was calculated after treatment of the sample with UV endonuclease and is corrected for loss of sc-DNA not resulting from dimers.

Table I. Average Intensities and Fluxes of 532-nm, 28-ps Pulses Used To Produce Dimers and the Resulting Values of Slope (F) and σ_2

av intensity, GW cm^{-2}	av flux × 10^{-27}, photons cm^{-2} s^{-1}	slope(F) × 10^{-5}	σ_2 × 10^{52} cm^4 s photons^{-1}
8.04	21.5	−7.56 ± 2.60	0.415
5.95	15.9	−2.30 ± 0.75	0.231
4.09	10.9	4.11 ± 0.39	0.875
3.20	8.58	−2.13 ± 0.19	0.740
1.91	5.12	−0.376 ± 0.071	0.365
1.49	3.98	−0.276 ± 0.031	0.443
1.03	2.76	−0.168 ± 0.103	0.560

where E is the energy per pulse in joules entering the sample, τ_p is the pulse duration (28-ps FWHM), $h\nu$ is the photon energy, and R_o is the capillary radius (0.075 cm), eq 2 can be rewritten as

$$\ln [f_{sc}(t)] = \ln [f_{sc}(t = 0)] - \sigma_2\phi_2\tau_p\alpha\beta\bar{F}^2N \quad (4)$$

where N is the number of laser pulses, and α and β are correction terms for the pulse shape and beam profile, respectively. Assuming that the intensity during one of the pulses is temporally and spatially described by a Gaussian distribution

$$F(r,\hat{t}) = F_{max} \exp[-4 \ln (2)\hat{t}^2/\tau_p^2] \exp[-\ln (2)r^2/R^2] \quad (5)$$

Using the values of the beam radius, R, and τ_p appropriate to our experiment, we can evaluate α and β by carrying out the integration in eq 2 over a single pulse. Because eq 5 describes a single pulse, $\hat{t}$ = time during the pulse with the center of the pulse as $\hat{t} = 0$. For our specific experimental parameters, $\alpha = 0.664$ and $\beta = 1.234$.

A representative plot of ln [$f_{sc}(t)$] versus N is shown in Figure 3 in which the average intensity was 3.20 GW/cm^2. Each data point in Figure 3 has been corrected for any strand breaks introduced by the irradiation that do not result from cleavage by UV endonuclease. Thus, the decrease in f_{sc} reflects only dimers introduced into the DNA by 532-nm radiation. The plots at all laser intensities were linear. Table I lists the slopes of these plots, slope($\bar{F}$).

If the formation of dimers results from a two-photon process, the plot of the ln [slope($\bar{F}$)] versus ln $\bar{F}$ should yield a straight line with a slope of 2 according to

$$\ln [\text{slope}(\bar{F})] = 2 \ln \bar{F} + \ln [\sigma_2\phi_2\tau_p\alpha\beta] \quad (6)$$

As shown in Figure 4 these data can be fitted by linear regression to a line with a slope of 1.88 ± 0.26, indicating that the dominant mechanism for dimer formation is indeed two-photon absorption.

Further evidence supporting dimer formation by a two-photon process rather than a one-proton absorption was obtained from a control experiment using low-intensity 514-nm radiation from an argon ion laser. Samples of sc-DNA exposed to up to 7 J of 514-nm radiation did not show an increase the conversion of sc-DNA to rel-DNA upon treatment with UV endonuclease.

Strand breaks were introduced into sc-DNA by both high-intensity 532-nm and low-intensity 514-nm radiation in samples not

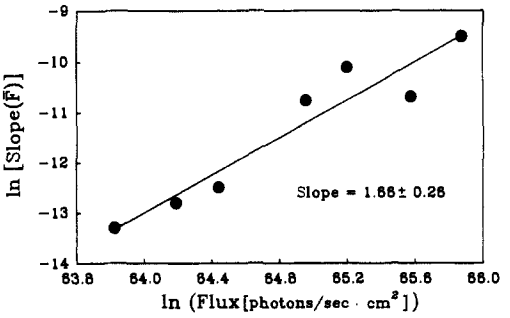

Figure 4. Relationship between efficiency of dimer formation and photon flux with 532-nm, 28-ps pulses.

treated with UV endonuclease. The most reasonable mechanism for the formation of these strand breaks is that the DNA samples contain a low concentration of a photosensitizer capable of initiating strand breaks. Although this absorber was not identified, it is known that many visible-absorbing organic and organometallic compounds photosensitize the formation of DNA breaks with varying efficiencies.[15] In samples exposed to the same number of photons at high and low intensities, a greater number of DNA strand breaks were produced by the high intensities. These strand breaks are not caused by the radical or mechanical mechanisms discussed below because optical breakdown was not detected even at the highest intensities used. Possibly the photosensitizer causes strand breaks after one-photon absorption and after sequential two-photon absorption. As noted above, the data presented in Figure 3 and Table I have been corrected for strand breaks formed by this photosensitization process.

Two-Photon Absorption Cross Section for DNA at 532 nm. A calculation of the two-photon cross section was made from the slope of the ln [$f_{sc}(t)$] versus N plots at each intensity and the results are listed in Table I. The quantum yield, Φ_2, for production of a dimer after two-photon absorption was assumed to be the same as the quantum yield for production of a dimer following absorption of one UV photon by pBR322 DNA. A value of 0.02 was used for Φ_1.[12]

An average for σ_2 (±SEM) of 0.5 (±0.4) × 10^{-52} cm^4 s photon^{-1} per nucleotide was obtained from data at seven intensities. The value of σ_2 obtained is relatively low for a two-photon cross section; values of (1–20) × 10^{-50} cm^4 s photon^{-1} are more typically reported.[8] There is no obvious reason why nucleotide should have low values of σ_2. The σ_1 for nucleotides and aromatic hydrocarbons are comparable at their respective absorption maxima but values of 5 × 10^{-51}–4 × 10^{-50} cm^4 s photon^{-1} for σ_2 have been reported for the latter.[9]

Possible sources of error that would give low values for σ_2 involve the assumptions that $\Phi_1 = 0.02$ and that $\Phi_1 = \Phi_2$. The value for Φ_1 was based on measurements with linear DNA rather than on sc-DNA. Because sc-DNA is highly twisted and more rigid than linear DNA, two adjacent pyrimidines may not be able to attain the proper orientation to form a cyclobutyl ring as easily in sc-DNA as in linear DNA. This would lead to a lower value for Φ_1 and, thus, a higher value for σ_2. However, this topographical difference between DNA molecules is unlikely to account for the 2 orders of magnitude lower value for σ_2 obtained in this study. The other assumption, that $\Phi_1 = \Phi_2$, must also be considered. Simultaneous two-photon absorption excites molecules to a different electronic state (one with the same parity as the ground state) that does one-photon absorption. Because the two states are very close in energy and are expected to relax to the lowest electronically excited state very rapidly, it is improbable that Φ_2 would be significantly different from Φ_1.

Calculation of a two-photon cross section for absorption from measurements of the yield of a product has the advantage of being integrative; thus, even low probability processes can be detected and quantitated. Fluorescence measurements are generally used to obtain σ_2 values but cannot be used for many molecules, including DNA, because of their very low fluorescence quantum yields. Fluorescence also has the disadvantages of being subject

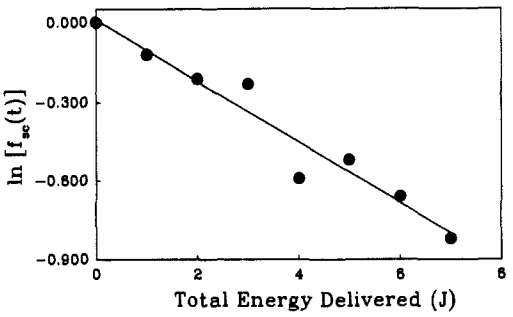

Figure 5. Formation of strand breaks in pBR322 DNA induced by 532-nm, 28-ps pulses under conditions resulting in optical breakdown on every pulse at 2 mJ/pulse. The fraction of DNA remaining at sc-DNA (f_{sc}) after delivery of varying numbers of pulses was corrected for strand breaks present before irradiation.

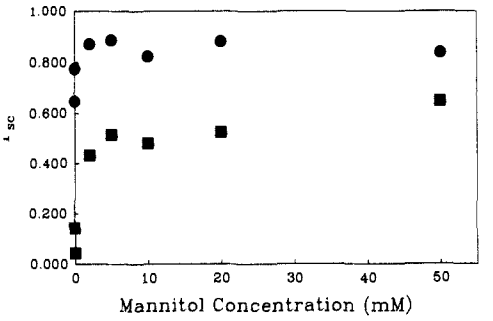

Figure 6. Effect of mannitol on the decrease in sc-DNA induced by 532-nm, 28-ps pulses under conditions resulting in optical breakdown on every pulse. Squares, 6 J total cumulative energy delivered; circles, 1.5 J total cumulative energy delivered.

to interference by very low levels of fluorescencing impurities and of requiring strict attention to the geometry of the experimental apparatus. The disadvantage of our method is that σ_2 is obtained by an indirect measurement of excited states. Thus, any unrecognized process altering the excited state population will influence the measured value.

DNA Strand Breaks Produced after Laser-Induced Plasma Formation. Tightly focusing the 28-ps pulses into the sample solutions caused optical breakdown (plasma formation) on every pulse. The ln f_{sc} measured without UV endonuclease treatment was plotted versus the number of laser pulses delivered. The results of a typical experiment using 2 mJ/pulse are shown in Figure 5. The maximum total delivered energy was 7 J (3500 laser pulses). On the basis of the number of photons or amount of energy delivered to the sample, the number of lesions produced in DNA was greater for laser-induced optical breakdown than that produced by two-photon absorption at 532 nm. For example, delivering 7 J (2 mJ/pulse) of focused 532-nm, 28-ps radiation decreased f_{sc} to 0.41 whereas delivering the same energy, using the collimated beam, also at ~2 mJ/pulse (I = 4.1 GW/cm^2) decreased f_{sc} only to 0.80. The difference is actually larger than this 2-fold difference in f_{sc} because the sample volume was 6.7-fold greater in the experiments with plasma formation although the DNA concentration was 2.5-fold lower.

Two mechanisms for initiation of strand breaks in DNA were considered, radical induced and mechanically induced. Water-derived radicals are created by the high-temperature plasma produced by optical breakdown and the collapse of the subsequent cavitation bubble. Hydroxy radicals are produced by ultrasound-induced cavitation bubbles.[20] The reactions of water-derived radicals with DNA have been extensively studied because of the involvement of these processes in ionizing radiation damage to DNA.[21] These radicals, particularly the hydroxy radical, initiate cleavage of the DNA backbone by adding to the bases of DNA and by abstracting hydrogens from the deoxyribose of the DNA backbone.[22] The second mechanism, mechanical disruption, is expected from the acoustic transients generated from the laser-induced plasma. The shock wave and acoustic wave may cause breaks in the DNA strands by mechanically disrupting the DNA backbone.

In order to distinguish between DNA strand breaks caused by radicals and those caused by mechanical mechanisms, radical quenchers were used. The inhibition of strand breaks by mannitol is shown in Figure 6 for cumulative energies of 1.5 and 6 J. The percent of strand breaks that was quenched by mannitol was only approximately 55–65%, indicating that both radical-initiated and mechanically induced strand breaks are important under our experimental conditions. Similar results were obtained when sodium azide was used to inhibit strand breaks. This result differs from that obtained in a study of the formation of strand breaks in DNA caused by the collapse of ultrasonically generated cavitation bubbles in which only ~20% of the single-strand breaks caused by cavitation bubbles were not quenchable by cysteamine.[23] The unquenchable portion was attributed to mechanical effects, which broke mainly single chains. The higher proportion of strand breaks found with laser-induced breakdown may be due to the fact that spatially localized pressure transients of at least several kilobars may be generated under our conditions.[11a]

In the analysis of some samples, linear DNA molecules were detected by gel electrophoresis, indicating that double-strand breaks had occurred in the sc-DNA. The yield of double-strand breaks was always less than 10% of the yield of single-strand breaks. Double-strand breaks could result from two independent, closely spaced single-strand breaks on opposite strands or from breakage of both strands simultaneously. The former is highly unlikely to occur because pBR322 DNA contains more than 4000 base pairs, so that two independent events occurring within ~10 base pairs of each other is improbable. The double-strand breaks are most likely caused by mechanical disruption due to the shock waves or acoustic waves.

Treatment of the irradiated samples with UV endonuclease did not increase the number of strand breaks, indicating that no dimers were formed. This result indicates that the radiation from the plasma, which is expected to be partially in the UV, was not absorbed by the DNA to produce detectable dimers.

Relevance to Use of High-Peak-Power Lasers in Biology and Medicine. Our results indicate that high-intensity visible radiation can initiate photochemistry in UV-absorbing biological molecules by nonresonant two-photon absorption and that laser-induced plasma causes damage to biomacromolecules. Specifically, visible light was shown to induce formation of mutagenic photoproducts (dimers) in DNA and cause DNA chain cleavage. We are extending these studies to bacteria to learn whether two-photon absorption by DNA causes biological responses.

In general, biological effects of nonresonant two-photon absorption are possible but are highly improbable under the conditions of most medical and biological applications of pulsed lasers. The use of two-photon absorption of lower energy radiation to produce the effect of a higher energy photon has the advantage that longer wavelengths have greater penetration into tissue but has the disadvantages of requiring high intensities and of low probability for absorption. Sequential two-photon absorption, especially that involving triplet states, occurs at much lower intensities and may be more useful in biology and medicine.

Acknowledgment. Support for this work from the MFEL program of SDIO under Contract N00014-86-K-0117 is gratefully acknowledged. We thank Joan Frisoli, Kevin Schomacker, Agnes Walsh, Gail Dalickas, and Gary Gofstein for their technical help and advice.

(20) Makino, K.; Mossoba, M. M.; Riesz, P. *J. Phys. Chem.* **1983**, *87*, 1369–1377.

(21) von Sonntag, C. *The Chemical Basis of Radiation Biology*; Taylor and Francis: London, 1987; pp 221–293.

(22) Deeble, D. J.; Schulz, D.; von Sonntag, C. *Int. J. Radiat. Biol.* **1986**, *49*, 915–926.

(23) Kondo, T.; Arai, S.-I.; Kuwabara, M.; Yoshii, G.; Kano, E. *Radiat. Res.* **1985**, *104*, 284–292.